



Personal identification based on handwriting

H.E.S. Said^{a,*}, T.N. Tan^b, K.D. Baker^a

^a*Department of Computer Science, University of Reading, Whiteknights, P.O.Box 225, Reading, Berkshire RG6 6AY, UK*

^b*National Laboratory of Pattern Recognition, Institute of Automation, Chinese Academy of Sciences, Beijing, People's Republic of China*

Received 24 June 1998; received in revised form 15 December 1998; accepted 15 December 1998

Abstract

Many techniques have been reported for handwriting-based writer identification. The majority of techniques assume that the written text is fixed (e.g., in signature verification). In this paper we attempt to eliminate this assumption by presenting a novel algorithm for automatic text-independent writer identification. Given that the handwriting of different people is often visually distinctive, we take a global approach based on texture analysis, where each writer's handwriting is regarded as a different texture. In principle, this allows us to apply any standard texture recognition algorithm for the task (e.g., the multi-channel Gabor filtering technique). Results of 96.0% accuracy on the classification of 1000 test documents from 40 writers are very promising. The method is shown to be robust to noise and contents.
© 1999 Pattern Recognition Society. Published by Elsevier Science Ltd. All rights reserved.

Keywords: Personal identification; Writer identification; Texture analysis; Gabor filters; Handwriting processing; Document image processing

1. Introduction

Signature verification has been an active research topic for several decades in the image processing and pattern recognition community [1]. Despite continuous effort, signature verification remains a challenging issue. It provides a way of identifying the writer of a piece of handwriting in order to verify the claimed identity in security and related applications. It requires the writer to write the same fixed text. In this sense, signature verification may also be called text-dependent writer verification (which is a special case of text-dependent writer identification where more than one writer has to be considered). In practice, the requirement and the use of fixed text makes writer verification prone to forgery. Furthermore, text-dependent writer identification is inapplicable in many important practical applications, for example,

the identification of the writers of archived handwritten documents, crime suspect identification in forensic sciences, etc. In these applications, the writer of a piece of handwriting is often identified by professional handwriting examiners (graphologists). Although human intervention in text-independent writer identification has been effective, it is costly and prone to fatigue.

Research into writer identification has been focused on two streams, off-line and on-line writer identification. On-line writer identification techniques are not well developed (as compared to on-line signature verification methods), and only a few papers (e.g. [2]) have been published on this subject. In comparison, off-line systems have been studied either as fully automated tools or as interactive tools. These systems are based on the use of computer image processing and pattern recognition techniques to solve the different types of problems encountered: pre-processing, feature extraction and selection, specimen comparison and performance evaluation.

This paper presents an off-line system based on computer image processing and pattern recognition techniques. There are two approaches to the off-line method,

*Corresponding author. Tel.: +44-118-987-51-23x7641; fax: +44-118-975-1994.

E-mail address: H.E.S.Said@reading.ac.uk (H.E.S. Said)

namely text-dependent and text-independent. Our work is a text-independent approach where a texture analysis technique is introduced. The text-independent approach uses feature sets whose components describe global statistical features extracted from the entire image of a text. Hence it may be called texture analysis approach.

Two general approaches have been proposed in the off-line method: Histogram descriptions and Fourier transform techniques. In the first case, the frequency distribution of different global and local properties is used [3]. Some of these properties are directly or indirectly related to specific features used in the forensic document analysis [4].

In the second case, Duvernoy et al. [5] have reported that the most important variation of the writers transfer function is reflected in the low-frequency band of Fourier spectrum of the handwriting images. Similarly, Kuckuck [6] has used Fourier transform techniques to process handwritten text as texture. The features extracted were either composed of sequences of spectrum mean values per bandwidth, polynomial fitting coefficients or a linear mapping of these coefficients. The method has been tested on a set of 800 handwriting samples (20 writers, 40 samples per writer). An overall classification rate of 90% for all features extracted was obtained.

This paper uses multichannel spatial filtering techniques to extract texture features from a handwritten text block. There are many filters available for use in the multichannel technique. In this paper we use Gabor filters, since they have proven to be successful in extracting features for similar applications [7–11]. We also use grey-scale co-occurrence matrices (GSCM) for feature extraction as a comparison. For classification two classifiers are adopted, namely the weighted Euclidean distance (WED) and the (K -NN) classifiers.

The subsequent sections describe the normalisation of the handwriting images, the extraction of writer features, the experimental results and finally the conclusions.

2. The new algorithm

The algorithm is based on texture analysis and is illustrated diagrammatically in Fig. 1. The three main stages are described in turn in the remainder of this section.

2.1. Normalisation of handwriting images

Texture analysis cannot be applied directly to handwriting images, as texture is affected by different word spacing, varying line spacing, etc. The influence of such factors is minimised by normalisation.

The input to this normalisation stage is a binary image of any handwritten document. The handwriting may contain lines of different point size and different spacing between lines, words and characters. The normalisation is performed as follows: Text lines are located using the horizontal projection profile [10]. Spaces between lines/words and margins are set to a predefined size. Then, incomplete lines are filled by means of text padding. Random non-overlapping blocks (of pixels) are then extracted from the normalised image. Texture analysis is applied to these blocks. Further details on normalisation may be found in [10]. The main steps are illustrated in Fig. 2 below.

2.2. Features extraction

In principle, any texture analysis technique can be applied to extract features from each uniform block of handwriting. Here two established methods are implemented to obtain texture features, namely the multichannel Gabor filtering technique (MGF) [12] and the grey-scale co-occurrence matrix (GSCM) [13]. The former is a popular method which is well recognised and the latter is often used as a benchmark in texture analysis [13].

2.2.1. Gabor filtering

The multichannel Gabor filtering technique is inspired by the psychophysical findings that the processing of pictorial information in the human visual cortex involves a set of parallel and quasi-independent mechanisms or cortical channels which can be modelled by bandpass filters. Mathematically the 2D Gabor filter can be expressed as follows:

$$h(x, y) = g(x, y)e^{-2\pi j(u_0x + v_0y)}, \quad (1)$$

where $g(x, y)$ is a 2-D Gaussian function of the form

$$g(x, y) = e^{1/2[(\alpha^2 + \beta^2)/\sigma^2]}. \quad (2)$$

A simple computational model for the cortical channels is described in [12]. Briefly stated, each cortical

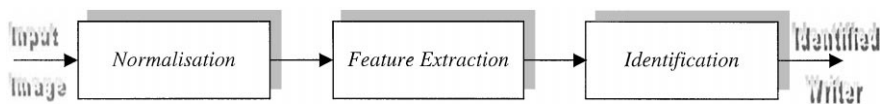


Fig. 1. Block diagram of the algorithm.

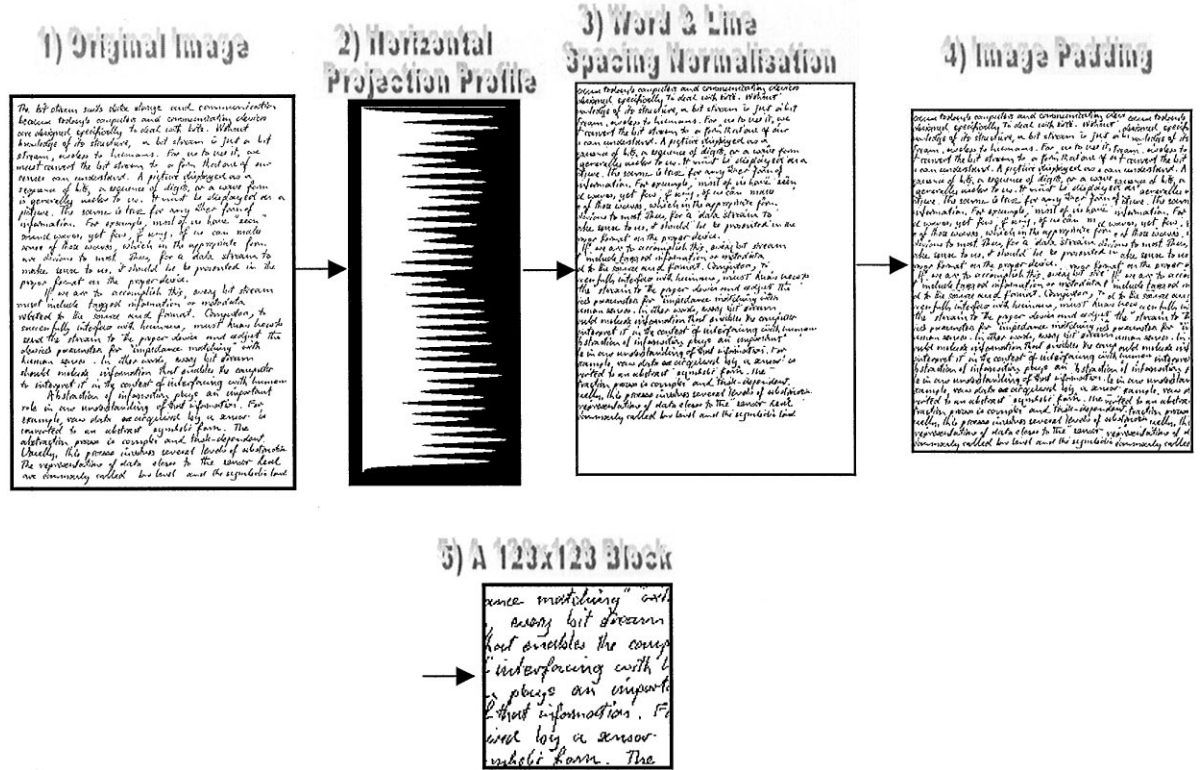


Fig. 2. The normalisation of the handwriting images.

channel is modelled by a pair of Gabor filters $h_e(x, y; f, \theta)$ and $h_o(x, y; f, \theta)$. The two Gabor filters are of opposite symmetry and are given by

$$h_e(x, y; f, \theta) = g(x, y)\cos(2\pi f(x \cos \theta + y \sin \theta)),$$

$$h_o(x, y; f, \theta) = g(x, y)\sin(2\pi f(x \cos \theta + y \sin \theta)). \quad (3)$$

The Fourier transform of the filter is calculated and the resultant output image is obtained using FFT, for example, if g_o the odd filters outputs then:

$$g_o(x, y) = \text{FFT}^{-1}[P(u, v)H_o(u, v)] \quad (4)$$

where $P(u, v)$ is the Fourier transform (FT) of the input image $p(x, y)$ and $H_o(u, v)$ is the FT of the filter $h_o(x, y; f, \theta)$. The results of the two given filters are combined using Eq. (5) and a single value at each pixel of the image is obtained (for justification see [8]).

$$q(x, y) = \sqrt{q_e^2(x, y) + q_o^2(x, y)}. \quad (5)$$

The two important parameters of the Gabor filter are and (the radial frequency and orientation, respectively), which define the location of the channel in the frequency plane. Commonly used frequencies are power of 2. In [12] it was shown that for any image of size $N \times N$, the

important frequency components are within $f \leq N/4$ cycles/degree.

In this paper we use frequencies of 4, 8, 16 and 32 cycles/degree. For each central frequency f , filtering is performed at $\theta = 0, 45^\circ, 90^\circ$, and 135° . This gives a total of 16 output images (four for each frequency) from which the writer's features are extracted. These features are the mean and the standard deviation of each output image (therefore, 32 features per input image are calculated). Testing was performed using either all 32 features or various sub-sets (e.g., features associated with a particular radial frequency).

2.2.2. Grey-scale co-occurrence matrices

GSCMs are also considered. Generally speaking, GSCMs are expensive to compute. For an image represented using N grey levels, each GSCM is of size $N \times N$. Binary handwriting images contain only two grey levels. It is therefore reasonable to use the GSCM technique.

In this paper, GSCMs were constructed for five distances ($d = 1, 2, 3, 4, 5$) and four directions $\alpha = (0, 45, 90, 135^\circ)$. This gives each input handwriting image 20 matrices of dimension 2×2 .

When the size of the GSCM is too large to allow the direct use of matrix elements, measurements such as

energy, entropy, contrast and correlation are computed from the matrix and used as features [13]. For each 2×2 GSCM derived from a binary handwriting image, there are only three independent values due to the diagonal symmetry. The three values are used directly as features. So we have 60 ($= 2\phi \times 3$) features per handwriting image.

2.3. Writer identification

Two classifiers were considered, namely the weighted Euclidean distance (WED) classifier and the K nearest-neighbour classifier (K -NN).

2.3.1. The weighted Euclidean distance classifier

Representative features for each writer are determined from the features extracted from training handwriting texts of the writer. Similar feature extraction operations are carried out, for an input handwritten text block by an unknown writer. The extracted features are then compared with the representative features of a set of known writers. The writer of the handwriting is identified as writer K by the WED classifier *iff* the following distance function is a minimum at K :

$$d(k) = \sum_{n=1}^N \frac{(f_n - f_n^k)^2}{(v_n^k)^2}, \quad (6)$$

where f_n is the n th feature of the input document, and f_n^k and v_n^k are the sample mean and sample standard deviation of the n th feature of writer k respectively.

2.3.2. The K nearest-neighbours classifier

When using the K nearest-neighbours classifier (K -NN), for each class V in the training set, the ideal feature vectors are given as f_v . Then we detect and measure the features of the unknown writer (represented as U). To determine the class R of the writer we measure the similarity with each class by computing the distance between the feature vector f_v and U . The distance measure used here is the Euclidean distance. Then the distance computed d_v of the unknown writer from class V is given by

$$d_v = \left[\sum_{j=1}^N (U_j - f_{vj})^2 \right]^{\frac{1}{2}}, \quad (7)$$

where $j = 1, \dots, N$ (N is the number of the features considered).

The writer is then assigned to the class R such that:

$$d_R = \min(d_v), \quad (8)$$

where ($k = 1, \dots$, no of classes). Other more sophisticated measures and classifiers such as neural network classifiers could have been used. The emphasis in this paper, however, is on computational simplicity.

3. Experimental results

A number of experiments were carried out to show the effectiveness of the proposed algorithms. Forty people were selected, then divided into two groups (each consist of 20 people). Examples of handwriting by these people are shown in Fig. 3.

For the purpose of the classification experiments 25 non-overlapping handwriting blocks were extracted for each person. Each sample was selected from an A4 page, scanned using a HP ScanJet4c in custom mode with extra heavy lighting, at a resolution of 150 dpi. The sample images were divided first into 10 training and 15 test images per writer (Set A) followed by 15 training and 10 test images (Set B). Images in the test sets did not appear in the training sets. Testing was conducted using different combinations of features under both classifiers.

3.1. Results from Gabor filtering

The effects of the Gabor filtering on classification were investigated. In Fig. 4, the primary images that were produced using channels at $f = 4, 8, 16, 32$ and $\theta = 0, 45, 90, 135^\circ$ are shown.

Tables 1–4 show the results of the multi-channel Gabor filter features using the two classifiers. It can be seen that features were extracted using the channels at $f = 4, 8, 16, 32$ and $\theta = 0, 45, 90, 135^\circ$ (hence a total of 32 features) and combination of different frequencies and orientation. The results from the weighted Euclidean distance (WED) were tabulated in Tables 1 and 3. In Tables 2 and 4 the results from the K nearest-neighbours classifier (K -NN) are given. The outcome of both classifiers is compared, and the results are shown in Figs. 5 and 6. Similar number of features were used for both classifiers.

When the WED classifier was used, generally higher identification accuracy were observed (especially for Set A). For example in Group 2, a classification rate of 96.0% was obtained when all 32 features were used (for Set B). Results of 96.0% were also observed when $f = 32$ and 16 were chosen (for Set A). It can be seen that the higher the channel frequency the better the classification accuracy. This effect is demonstrated clearly for both sets (Sets A and B).

Under the K -NN classifier, a classification rate of 77.0% was achieved when all features were used (for Set B). The best results (86.0%) under the K -NN were achieved for group1, when the frequencies of $f = 16$, and 32 were used (for Set B). For easier comparison Figs. 5 and 6 show the plots of the identification accuracies for the multi-channel Gabor filtering features under both classifiers, where the features sets are in the same order as in Tables 1–4 (e.g. features set 1 for all features; set 2 for all SD features, etc.). It can be easily be seen that filtering techniques using the WED classifier performs better.



Fig. 3. Handwriting examples of 30 different people.

3.2. Results from GSCM

In Tables 5-8, features were extracted using distances $d = 1, 2, 3, 4, 5$ and directions $\alpha = (0, 45, 90, 135^\circ)$ (there were a total of 60 features $(3 \times 5 \times 4)$). Different combinations of feature sets, e.g. features at $d = 1, 2, 3$ and four

directions (given above) were used (i.e. there were a total of 36 features $(3 \times 3 \times 4)$), etc.

Tables 5-8 show the classification rates for the GSCM approach under both classifiers. Here, the results can be seen to be much poorer than those for the multi-channel Gabor filtering method. This observation is consistent

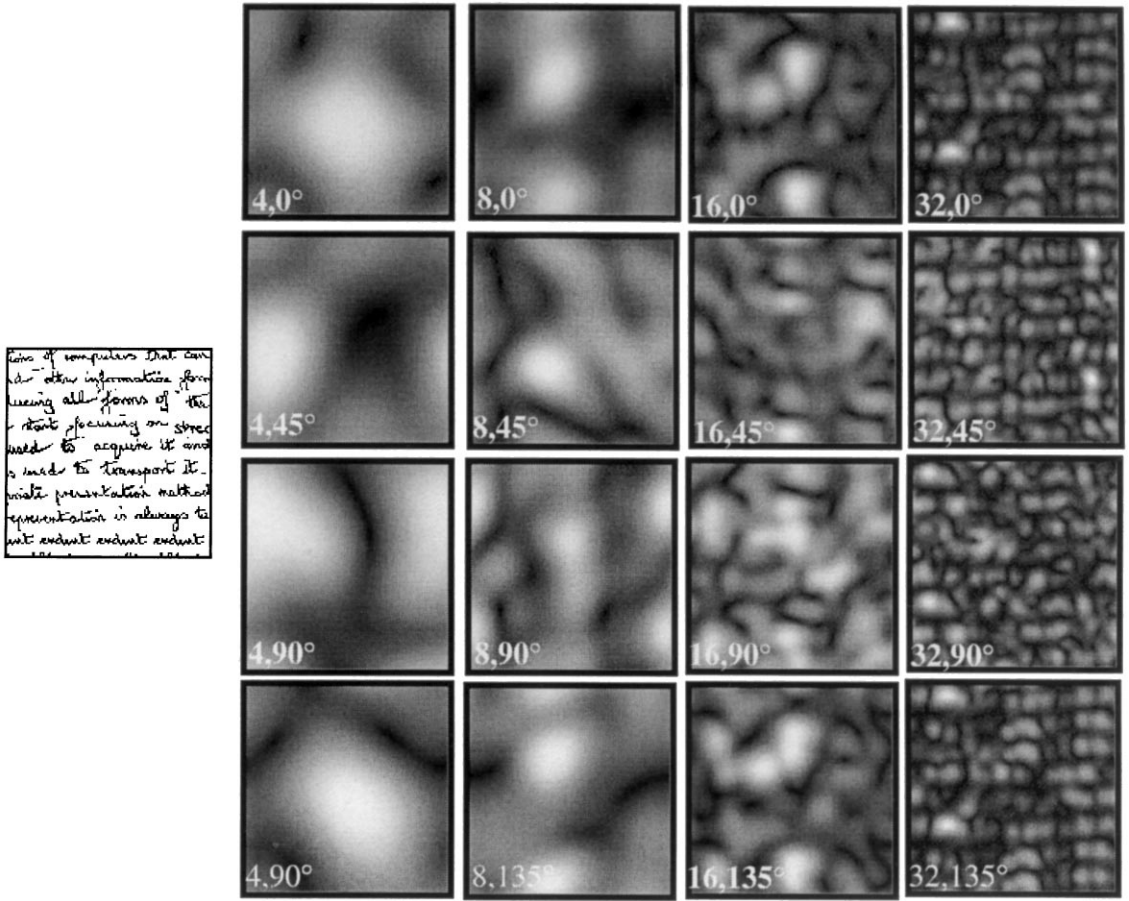


Fig. 4. The output images from the Gabor filter, at different frequencies and orientations for the first writer.

Table 1
Group 1: Identification accuracy of the Gabor filtering technique under WED

Features	All	SD	Mean	Mean at $f = 16, 32$	All at $f = 16, 32$	All at $f = 32$	All at $f = 16$	All at $f = 8$	All at $f = 4$
Set A	94.3	91.0	89.7	89.7	95.3	84.7	58.1	29.3	11.3
Set B	91.0	90.5	86.5	83.0	88.1	75.6	52.2	29.5	13.9

Table 2
Group 1: Identification accuracy of the Gabor filtering technique under K-NN

Features	All	SD	Mean	Mean at $f = 16, 32$	All at $f = 16, 32$	All at $f = 32$	All at $f = 16$	All at $f = 8$	All at $f = 4$
Set A	56.0	56.0	49.7	56.7	56.3	59.7	50.7	31.0	22.3
Set B	76.0	75.5	73.5	85.6	86.0	82.0	58.5	44.5	28.5

Table 3
Group 2: Identification accuracy of the Gabor filtering technique under WED

Features	All	SD	Mean	Mean at <i>f</i> = 16, 32	All at <i>f</i> = 16, 32	All at <i>f</i> = 32	All at <i>f</i> = 16	All at <i>f</i> = 8	All at <i>f</i> = 4
Set A	84.1	82.8	83.4	92.1	96.0	85.4	61.3	34.4	29.1
Set B	96.0	90.1	92.1	93.0	86.0	84.2	65.3	34.7	22.8

Table 4
Group 2: Identification accuracy of the Gabor filtering technique under K-NN

Features	All	SD	Mean	Mean at <i>f</i> = 16, 32	All at <i>f</i> = 16, 32	All at <i>f</i> = 32	All at <i>f</i> = 16	All at <i>f</i> = 8	All at <i>f</i> = 4
Set A	54.7	59.3	40.0	56.7	54.0	66.7	66.7	37.6	21.1
Set B	77.0	78.0	60.0	75.0	85.0	90.0	88.0	47.0	27.7

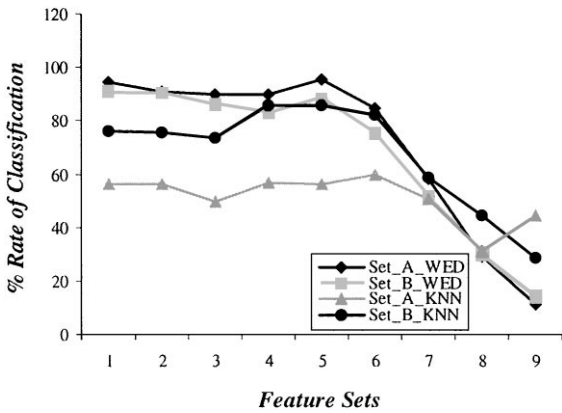


Fig. 5. Group 1: results from Gabor filter using the WED and K-NN classifier.

with the findings in [10,12]. Figs. 7 and 8 show plots of the identification accuracy for the GSCM features under both classifiers. The features sets appear in the same order as those in Tables 5–8.

The best results (shaded in the tables) show that only 72.2 and 63.6% (for groups 2 and 1, respectively) of the images were identified correctly when using the WED classifier, 36 texture features were required.

In comparison, a classification rate of 74.0 and 66.0% (for groups 2 and group 1, respectively) are obtained when the K-NN classifier was used (with a total of 24 texture features). Note that under the K-NN performance in Set B (using 10 testing images) is far better than Set A.

3.3. Performance evaluation

3.3.1. Sample invariance

The remarkable effectiveness of using multi-channel Gabor filtering technique for identification is partially due to the writer texture samples invariance. For this

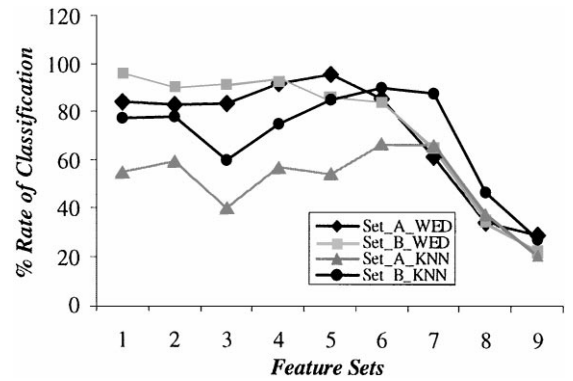


Fig. 6. Group 2: results from Gabor filter using the WED and K-NN classifier.

reason the relative sample invariance might be a useful parameter to compute. Writer sample invariance for different writers can be easily be calculated as follows:

$$\text{Sample invariance} = \frac{\text{writer sample SD}}{\text{writer sample mean}} \times 100. \quad (9)$$

The relative sample invariance can be calculated by means of the ratio of the standard deviation (SD) of writer sample features to the mean of those sample features. Table 9 shows the statistics for the proposed algorithms, the multi-channel Gabor filtering (MGF) and the GSCM. The results shown in Figs. 9–11 are given for 10 writers. It can be easily seen that MGF gave the best-sample invariance.

3.3.2. Types I and II errors

The task of verifying a writer is essentially that of recognising a genuine writer while rejecting the imitations. The performance of a system in achieving this is

Table 5
Group 1: Identification accuracy of the GSCM technique under WED

Distances	$d = 1, 2, 3, 4, 5$	$d = 1, 2, 3$	$d = 2, 3, 4$	$d = 3, 4, 5$	$d = 1, 2$	$d = 4, 5$	$d = 1$	$d = 4$
Set A	59.8	63.6	53.5	45.6	56.0	43.2	59.4	41.8
Set B	52.2	58.8	50.0	46.0	56.4	46.4	59.5	46.0

Table 6
Group 1: Identification accuracy of the GSCM technique under K-NN

Distances	$d = 1, 2, 3, 4, 5$	$d = 1, 2, 3$	$d = 2, 3, 4$	$d = 3, 4, 5$	$d = 1, 2$	$d = 4, 5$	$d = 1$	$d = 4$
Set A	43.3	45.3	40.3	39.7	37.7	37.3	44.3	38.3
Set B	60.5	68.0	57.0	54.0	74.0	53.5	62.5	58.5

Table 7
Group 2: Identification accuracy of the GSCM technique under WED

Distances	$d = 1, 2, 3, 4, 5$	$d = 1, 2, 3$	$d = 2, 3, 4$	$d = 3, 4, 5$	$d = 1, 2$	$d = 4, 5$	$d = 1$	$d = 4$
Set A	65.1	72.2	67.6	57.0	71.5	58.3	76.8	57.0
Set B	71.0	65.2	75.8	60.4	62.2	60.4	73.3	59.4

Table 8
Group 2: Identification accuracy of the GSCM technique under K-NN

Distances	$d = 1, 2, 3, 4, 5$	$d = 1, 2, 3$	$d = 2, 3, 4$	$d = 3, 4, 5$	$d = 1, 2$	$d = 4, 5$	$d = 1$	$d = 4$
Set A	50.7	64.0	58.7	51.3	62.0	31.4	61.3	31.4
Set B	63.0	75.0	66.0	60.0	66.0	49.5	60.0	56.0

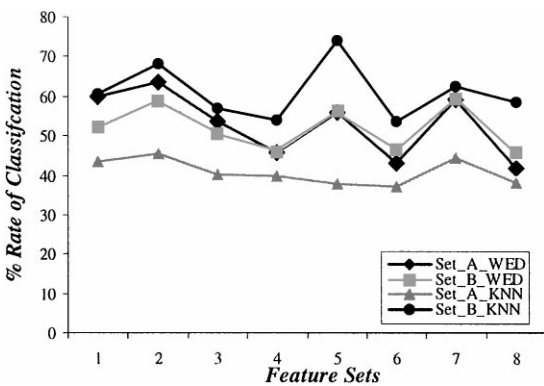


Fig. 7. Group 1: results from GSCM using the WED and K-NN classifiers.

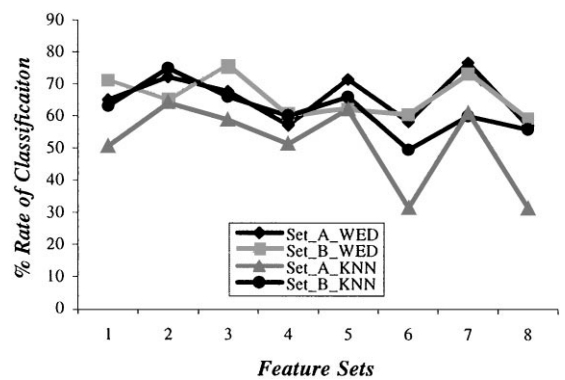


Fig. 8. Group 2: results from GSCM using the WED and K-NN classifiers.

measured in two ways, false rejection of genuine writers and false acceptance of imitations. These two measures are termed types I and II errors, respectively. The performance of any verification systems is often characterised

by the combinations of types I and II errors into an overall performance measure, known as the equal error rate, the error is calculated when type I error is equal to Type II error [14].

Table 9
Group 2: The deviation-to-mean ratios of Gabor filtering and GSCM technique

Writer	1	2	3	4	5	6	7	8	9	10
MGF	1.04	0.89	0.94	0.92	0.92	0.91	0.98	1.02	0.92	0.93
GSCM	1.93	2.04	1.95	1.89	2.03	1.95	1.82	1.94	1.93	1.99

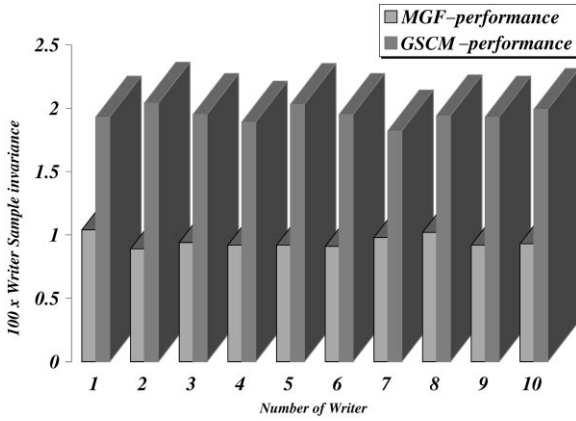


Fig. 9. The performance of the MGF and GSCM techniques.

The equal error rate is calculated for the optimum identification rates for the Gabor filtering and GSCM techniques that shown in Tables 1–8. The results of the equal error rate are shown in Tables 10–13. It can be seen that the best error rate given is 0.57% for the MGF technique using the WED classifier, where all the features were considered. In comparison an error rate of 2.32% for GSCM technique is obtained for the WED classifier, and that using a distance $d = 1, 2, 3$ for Set B.

3.4. Remarks

It is clear that the identification accuracy is much higher when the Gabor filter technique is used. Poor results are shown for the GSCM method.

In summary, the following observations can be made based on the results presented above:

1. Under all circumstances the multichannel filtering technique outperforms the GSCM technique (although computationally it is more expensive).
2. The overall performance of the WED classifier appears to be better than that of the K-NN.
3. It has also been noted that Set A gave higher identification accuracy when the WED is used, but Set B recorded better identification results when the K-NN classifier is used.
4. The results have clearly demonstrated the potential of the proposed texture based approach to personal identification from handwriting images.

4. Future work

The approach that has been adopted here is mainly text-independent. In the future text-dependent writer identification will be introduced. This will cover writer signature verification approaches. A comparison between the two approaches will then be drawn.

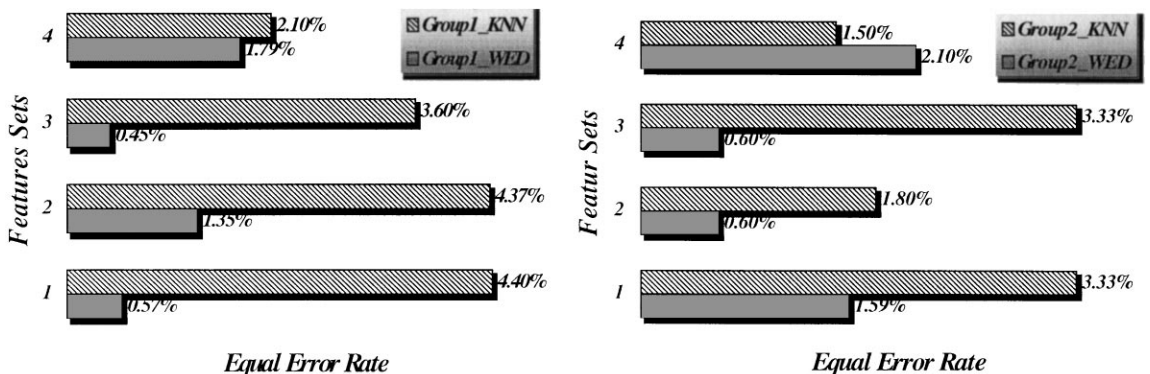


Fig. 10. The equal error rates for groups 1 and 2 using GFM technique.

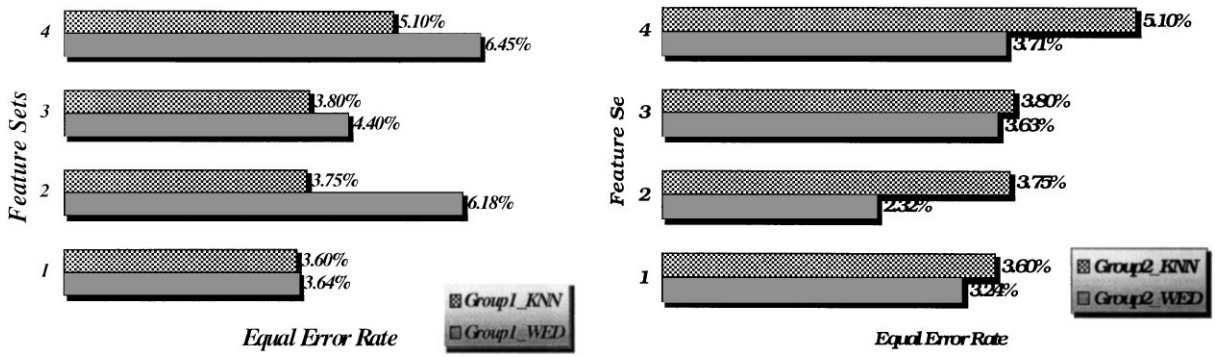


Fig. 11. The equal error rates for groups 1 and 2 using GSCM technique.

Table 10

Group 1: Error rate of the Gabor filtering technique under K-NN and WED classifiers

Classifier	The WED		The K-NN	
	All	All at $f = 16, 32$	All	All at $f = 16, 32$
Set A	0.57%	0.45%	4.4%	3.6%
Set B	1.35%	1.79%	4.37%	2.1%

Table 11

Group 2: Error rate of the Gabor filtering technique under K-NN and WED classifiers

Classifier	The WED		The K-NN	
	All	All at $f = 16, 32$	All	All at $f = 16, 32$
Set A	1.59%	0.6%	3.33%	3.33%
Set B	0.6%	2.1%	1.8%	1.5%

Table 12

Group 1: Error rate of the GSCM technique under K-NN and WED classifiers

Classifier	The WED		The K-NN	
	$d = 1, 2, 3$	$d = 1, 2$	$d = 1, 2, 3$	$d = 1, 2$
Set A	3.64%	4.4%	5.47%	4.8%
Set B	6.18%	6.45%	4.8%	3.9%

Table 13

Group 2: Error rate of the GSCM technique under K-NN and WED classifiers

Classifier	The WED		The K-NN	
	$d = 1, 2, 3$	$d = 1, 2$	$d = 1, 2, 3$	$d = 1, 2$
Set A	3.24%	3.63%	3.6%	3.8%
Set B	2.32%	3.71%	3.75%	5.1%

Currently our work is based on the extraction of global features, but further work will focus on the use of local features. An integrated system will be considered to combine both local and global features to produce more reliable classification accuracy.

Other work on writer identification might include the normalisation or the pre-processing of the skewed handwriting images [15]. In this field, work to detect the skewed angles of writer's documents is in progress. Research on skewed angle detection of printed document images has extensively been introduced in the field of document analysis, but little has been achieved for handwritten documents [16–18].

5. Conclusion

We have described a new approach for handwriting based personal identification. Most existing approaches assume implicitly that handwritten texts are fixed. The novel approach introduced in this paper eliminates such an assumption. The algorithm is based on the observation that the handwriting of different people is visually distinctive and a global approach based on textures analysis can be adopted. The approach is therefore text or content independent.

A number of experiments have been conducted which use 40 different writer classes. Features were extracted from handwriting images using the multi-channel Gabor filtering technique and the grey-scale co-occurrence matrix (GSCM) technique. Identification was performed using two different classifiers namely the weighted Euclidean distance (WED) and the K -nearest neighbours (K -NN) classifiers. The Results achieved were very promising, and an identification accuracy of 96.0% was obtained using the WED classifier. The K -NN classifier gave comparatively poor results.

Several factors affect the performance of such global approaches, including graphics and skewed handwriting. Other factors include the handwriting styles of different people, and similarities between different handwriting (see Fig. 1). We are currently investigating ways of reducing the impact of such factors on the performance of the proposed global approach. We will also consider local approaches which seek writer specific features to improve the recognition accuracy. In the future, both global and local approaches will be integrated as one system for better identification accuracy.

References

- [1] R. Plamondon, G. Lorette, Automatic signature verification and writer identification—the state of art, *Pattern Recognition* 22 (2) (1989) 107–131.
- [2] F.J. Maarse, L.R.B. Schomaker, H.L. Teulings, in: G.C. van der Vier, G. Mulder (Eds.), *Automatic Identification of Writers in Human–Computer Interaction: Psychonomic Aspects*, Springer, Heidelberg, 1986.
- [3] B. Azari, Automatic handwriting identification based on the external properties of the samples, *IEEE Trans. Systems Man Cybernet* 13 (1983) 635–642.
- [4] V. Klement, K. Steine, R. Naske, The application of image processing and pattern recognition techniques to the forensic analysis of handwriting, in: *Proceedings of the International Conference Security Through Science and Engineering*, West Berlin, 1980 pp. 5–11.
- [5] J. Duvernoy, Handwriting synthesis and classification by means of space-variant transform and Karhunen–Loeve analysis, *J. Opt. Soc. Am.* 65 (1975) 1331–1336.
- [6] W. Kuckuck, Writer recognition by spectra analysis, in: *Proceedings of the International Conference On Security Through Science Engineering*, West Berlin, Germany, 1980 pp. 1–3.
- [7] T.N. Tan, Written language recognition based on texture analysis, in: *Proceedings of the IEEE ICIP'96*, Lausanne, Switzerland, vol. 2, September 1996, pp. 185–188.
- [8] T.N. Tan, Texture edge detection by modelling visual cortical channels, *Pattern Recognition* 28 (9) (1995) 1283–1298.
- [9] A.K. Jain, S. Bhattacharjee, Text segmentation using Gabor filters for automatic document processing, *Mach. Vision Appl.* (1992) 169–184.
- [10] G.S. Peake, T.N. Tan, Script and language identification from document images, in: *Proceedings of the BMVC '97*, Essex, UK, vol. 2, September 1997, pp. 610–619.
- [11] T.R. Reed, J.M. Hans Du Buf, A review of recent texture segmentation and feature extraction techniques, *CVGIP: Image Understanding* 57 (1993) 359–372.
- [12] T.N. Tan, Texture feature extraction via visual cortical channel modelling, in: *Proceedings of the 11th IAPR International Conference Pattern Recognition* vol. III, 1992, pp. 607–610.
- [13] R.M. Haralick, Statistical and structural approaches to textures, *Proc. IEEE*, vol. 67, 1979, pp. 786–804.
- [14] M. Golfarelli, D. Maio, D. Maltoni, On error-reject trade-off in biometric verification systems, *IEEE Trans. Pattern Anal. Mach. Intel.* 19 (7) (1997) 786–796.
- [15] H.E.S. Said, G.S. Peake, T.N. Tan, K.D. Baker, Writer identification from non-uniformly skewed handwriting images, in: *The Proceedings of the British Machine Vision Conference BMVC98*, vol. 2, 1998, pp. 478–487.
- [16] D.S. Le, G.R. Thoma, H. Wechsler, Automatic orientation and skew angle detection for binary document images, *Pattern Recognition* 27 (10) (1994) 1325–1344.
- [17] H. S Baird, The skew angle of printed documents, *Proc. SPIE*, vol. 40, 1987, pp. 21–24.
- [18] W. Postal, Detection of linear oblique structures and skew in digitised documents, in: *Proceedings of the ICPR'86*, 1986, pp. 464–468.

About the Author—HUWIDA SAID received a B.Eng. honours degree in Electrical and Electronic Engineering from The University of Wales, Swansea in 1995. She is currently writing up for a PhD at The University of Reading and will graduate in July 1999. Her research interest include personal identification from facial features, handwritten characters and audio features. She is an associated member of the IEE and a member of the BCS.

About the Author—TIENIU TAN received his B.Sc. (1984) in Electronic Engineering from Xi'an Jiaotong University, China, and M.Sc. (1986), DIC (1986) and Ph.D. (1989) in Electronic Engineering from Imperial College of Science, Technology and Medicine, London, England.

In October 1989, he joined the Computational Vision Group at the Department of Computer Science, The University of Reading, England, where he worked as Research Fellow, Senior Research Fellow and Lecturer. In January 1998, he returned to China to take up a professorship at the National Laboratory of Pattern Recognition located at the Institute of Automation of the Chinese Academy of Sciences, Beijing, China.

Dr. Tan has published widely on image analysis and computer vision. He is a Senior Member of the IEEE and an elected member of the Executive Committee of the British Machine Vision Association and Society for Pattern Recognition (BMVA). He is the Asia Editor of the International Journal of Image and Vision Computing and an Associated Editor of the Pattern Recognition journal. His current research interests include speech and image processing, machine and computer vision, pattern recognition, multimedia, and robotics.

About the Author—KEITH BAKER Studied both Electronics Engineering and Mathematical Physics at the undergraduate level before receiving the PhD degree in physics in 1969 from the University of Sussex, Brighton, England.

After a period as postdoctoral fellow, he worked as a Systems Analyst on real-time air traffic control systems with the Software Systems Division of the Plessey Company. Later he was with the Burroughs Corporation, Detroit, MI, as a Supervisor of Software Engineering and Project Manager.

He has also spent some time as Lecture in Computer Science at the University of Sussex before taking up an appointment as Professor of Information Engineering Systems and head of the Electrical and Electronic Engineering Department at the University of Plymouth, England. In 1986 he moved to the University of Reading as full Professor of Computer Science, later to become the head of the Computer Science Department. He is Currently Dean of the Faculty of Sciences. His research interest include contributions to software engineering, computer vision, and intelligent systems.

Dr. Baker is the Editor-in Chief of the international *Journal Image and Vision Computing*, a Fellow of the IEE, and a member of the IEEE, the ACM and BCS.